Supplementary material

Supplement 1: Supplementary Figure legends

Supplementary Figure 1. Interquartile ranges of the complete ensemble given an initial viral aliquot of 50 pfu (sublethal) for all variables in the system. The black line shows the median of the trajectories at each time point, the dark grey shows the range from 25% of trajectories above and below the median, and the light grey shows the range from 5% to 95%. Black crosses indicate the mean and standard deviation of the experimental data for each analyte.

Supplementary Figure 2. Ensemble fit of Objectives. Plot of the posterior distribution of parameters in the space of objective values, which give the relative error of the fit of the model with a specific parameter set to either sublethal or lethal data. The solid curve represents Pareto boundary of the most optimal multi-objective fit values.

Supplementary Figure 3. Interquartile ranges of the complete ensemble given an initial viral aliquot of 500 pfu/ml (lethal) for all variables in the system. The black line shows the median of the trajectories at each time point, the dark grey shows the range from 25% of trajectories above and below the median, and the light grey shows the range from 5% to 95%. Black crosses indicate the mean and standard deviation of the experimental data for each analyte.

Supplementary Figure 4. Marginal distributions of the parameters obtained from the posterior distribution constituting the ensemble used to generate the interquartile graphs and predictions, shown within their respective ranges.

Supplement 2: Full Description of Equations

The full system of ordinary differential equations implements the biological processes described in Figure 1 of the manuscript. A justification of each equation follows.

$$\bar{N}' = \frac{b_{nt} T}{a_{nt} + a_{nl} L + T} - \frac{g_{nc} \bar{N} C}{a_{nc} + C} - \mu_{\bar{N}} \bar{N}$$

$$N' = \frac{g_{nc} \bar{N} C}{a_{nc} + C} - \mu_n N$$

$$M' = \frac{b_{mc} C^{h_c}}{a_{mc}^{h_c} + C^{h_c}} - \mu_M (M - b_m)$$

$$L' = \frac{b_l M \Sigma_1}{\Sigma_1 + \left(\frac{g_1 L + g_2}{L + d_2} \right)} - \mu_l (L - b_{lh} (1 - R_F) H)$$

$$T' = \frac{b_t M \Sigma_2}{\Sigma_2 + \left(\Sigma_2 + \frac{g_1 L + g_2}{L + d_2} \right) \left(\frac{k_1 L + k_2}{L + d_1} \right)} - \mu_t T$$

$$X' = \frac{b_{xn} N}{a_{xn} + N} - g_{xh} HX - g_{xi} IX - \mu_x X$$

$$A' = b_a + b_{ab} B - g_{av} AV - \mu_a A$$

$$C' = \frac{b_c M \Sigma_1}{\Sigma_1 + \left(\frac{g_1 L + g_2}{L + d_2} \right)} - \mu_c C$$

$$I' = g_{HV} VH - \frac{g_{ix} IX^{h_x}}{a_{ix}^{h_x} + X^{h_x}} - b_{ik} R_F IK - b_{ie} R_F IE - \mu_i (1 - R_F) I$$

$$H' = b_h H (1 - R_F) (D_H + D_I) \left(\frac{H - \theta}{H_0} \right) - g_{hv} VH - \frac{g_{hx} HX^{h_x}}{a_{hx}^{h_x} + X^{h_x}}$$

$$F' = b_{fi} (1 - R_F) I + b_{fp} P - g_{fi} IF - \mu_f F$$

$$V' = g_{vi} (1 - R_F) I - g_{vh} HV - \frac{g_v V}{1 + a_v V} - g_{va} AV - \mu_v V$$

$$D_H' = \frac{g_{hx} HX^{h_x}}{a_{hx}^{h_x} + X^{h_x}} - b_h (H) (1 - R_F) (D_H) \left(\frac{H - \theta}{H_{\max}} \right)$$

$$E' = \frac{b_{ep} P^{h_e}}{a_{ep}^{h_e} + P^{h_e}} - b_{ei} R_F IE - \mu_e E$$

$$B' = b_b + b_{bp} W P (B_{\max} - B) - \mu_b B$$

$$K' = b_k + \frac{b_{kc} C^{h_k}}{a_{kc}^{h_k} + C^{h_k}} - g_{ki} R_F IK - \mu_k K$$

$$P' = P_0\left(\frac{g_{pv}V}{a_{pv}+V} + g_{pd}D_I\right)\left(g_p + \frac{b_{pg}G}{a_{pg}+G}\right) - \mu_p(P - b_p)$$

$$W' = b_w + \frac{b_{wo}O}{a_{wo}+O}P - \mu_w W$$

$$G' = \frac{b_{go}W + g_{go}}{a_{go}+W}O + \frac{b_{gk}W + g_{gk}}{a_{gk}+W}K - \mu_g G$$

$$O' = \frac{b_{op}P^{h_o}}{a_{op}{}^{h_o} + P^{h_o}} - \mu_o O$$

where

$$\Sigma_1 = a_{11}T + a_{12}D$$

$$\Sigma_2 = a_{11}T + a_{12}D + \frac{a_{21}V}{a_{22}+V}$$

$$H_{\max} = H + I + D_H + D_I$$

$$R_F = F/(a_{rf} + F)$$

Initial Conditions

$$\tilde{N}_0 = 0$$
$$N_0 = 0$$
$$\mathrm{M}_0 = \mathrm{b}_m$$
$$\mathrm{L}_0 = \mathrm{b}_{lh}\mathrm{H}_{\max}$$
$$T_0 = 0$$
$$X_0 = 0$$
$$\mathrm{A}_0 = (\mathrm{b}_a + \mathrm{b}_{ab}\,\mathrm{B}_0)/\mu_a$$
$$C_0 = 0$$
$$I_0 = 0$$
$$H_0 = H_{\max}$$
$$\mathrm{F}_0 = \mathrm{b}_p\, {}^{b_{fp}}\!/_{\mu_f}$$
$$D_{H,0} = 0$$
$$\mathrm{E}_0 = \left({}^{\mathrm{b}_{ep}}\!/_{\mu_e}\right)\left(b_p^{h_e}\right)/\left(b_p^{h_e} + a_{ep}^{h_e}\right)$$
$$\mathrm{B}_0 = \left(\mathrm{b}_b + \mathrm{b}_{bp}\mathrm{b}_p\mathrm{W}_0\mathrm{b}_0\right)/\left(\mathrm{b}_{bp}\mathrm{b}_p\mathrm{W}_0 + \mu_b\right)$$
$$\mathrm{K}_0 = \mathrm{b}_k$$
$$\mathrm{P}_0 = \mathrm{b}_p$$
$$\mathrm{W}_0 = \left({}^{\mathrm{b}_p}\!/_{\mu_w}\right)\left(\mathrm{b}_{wo}\mathrm{O}_0\right)/\left(O_0 + a_{wo}\right)$$
$$\mathrm{G}_0 = \left({}^{\mathrm{O}_0}\!/_{\mu_g}\right)\left(\mathrm{b}_{go}\mathrm{W}_0\right)/\left(W_0 + a_{go}\right) + \left({}^{\mathrm{K}_0}\!/_{\mu_g}\right)\left(\mathrm{b}_{gk}\mathrm{W}_0\right)/\left(W_0 + a_{gk}\right)$$
$$\mathrm{O}_0 = \left({}^{\mathrm{b}_{op}}\!/_{\mu_o}\right)\left(b_p^{h_o}\right)/\left(b_p^{h_o} + a_{op}^{h_o}\right)$$

Neutrophils are modeled with a two-stage activation to become viable within the system. First, resting neutrophils (Ñ) require activation by TNF to become activated neutrophils (Ñ), inhibited by IL-10. Second, there must be a sufficient chemokine gradient for activated neutrophils to fully enter the tissue from nearby blood vessels. Neutrophils produce several factors (X) that eliminate invading organisms such as ROS, but this is toxic to the epithelial tissue as well. During a viral infection, the presence of neutrophils damages tissue without the benefit of targeting infected cells [2,11,58].

Macrophages (M) are comprised of two groups: alveolar macrophages that exist endemically within the epithelial tissue and act as sentries against foreign substances and organisms, and macrophages that enter the lung from blood via a chemokine gradient,

represented by a Hill term. They are deactivated on the time scale of days [59]. Macrophages receive a chemical signal in order to produce cytokines, e.g. LPS, IL-1. It is assumed cytokine production in macrophages is upregulated by pro-inflammatory signals Σ_1 and Σ_2. For simplicity, Σ_1 is taken to be a linear combination pro-inflammatory cytokine concentration and damaged tissue marker, while Σ_2 also includes the virus level [60].

In the steady state, epithelial tissue in the lung produces IL-10 (L); this maintains a moderately anti-inflammatory milieu for the lung tissue which is responsible for gas exchange. When the epithelial tissue dies or is exposed to type I interferons, epithelial cells produce less IL-10 and production shifts to macrophages. Macrophages produce IL-10 in a manner similar to the production of chemokines. IL-10 decays naturally on the order of hours.

Production of the signaling protein TNF (T) occurs based on exposure of macrophages to the presences of viral particles, exogenous TNF, and dead cells. This signaling is represented by the signal Σ_2. Since TNF is potentially dangerous to tissue due to its pro-inflammatory properties, IL-10 severely inhibits its production. In the Michaelis-Menten schema, both the maximal production and the substrate affinity are modulated by the inhibitor IL-10. TNF half-life is on the order of minutes [61].

Reactive oxygen species (X) are produced by activated neutrophils. These molecules interact with both healthy epithelial cells (H) and infected epithelial cells (I), causing damage to the tissue [62]. The free radicals have a very short half-life and decay naturally.

Free antibodies (A) are produced proportionally to B cells (B). There is also a small non-specific production term incorporated to production. The removal of several antibodies is required to achieve the removal of a single free virion. Antibodies have a long half-life and decay naturally [53].

The production of chemokines (C) is modeled as a Michaelis-Menten function of the signal Σ_1 multiplied by the number of macrophages. The Michaelis-Menten term is used to

represent the receptor saturation in macrophages; further, the substrate affinity term in the denominator of the Michaelis-Menten term is a saturating function of IL-10 that inhibits chemokine production. The half-life of chemokines is on the order of minutes [63].

Infected cells (I) do not undergo mitosis, and their numbers rise only by new infections. Their ability to produce new virions and to burst is inhibited by exposure to type I interferons. Elimination of infected cells comes from lysis by natural killer cells and CD 8^+ T cells. Since type I interferons cause heightened presentation on the cell surface, the elimination terms are multiplied by the exposure level. They are slightly more susceptible to death by neutrophil factors than their uninfected counterparts, independent of interferons.

Uninfected and undamaged epithelial target cells (H) regularly divide by mitosis when nearby cells are dead or damaged. However, exposure to type I interferons stops cellular machinery and halts mitosis. The mitosis is limited by contact inhibition in the presence of a high cell population and a strong Allee term in absence of other epithelial cells [64]. The strong Allee term is set near zero and provides for stability of the lethal state and ensures that fractional cell numbers do not divide. Uninfected target cells become infected by exposure to virus, and die when saturated by neutrophil factors.

Type I interferons (F) are produced by infected cells not significantly exposed to the interferons. In practice, this means that type I interferons along with TNF are the first responses the overall system has to the presence of virus. Additionally, antigen presenting cells (P) produce type I interferons. They are removed from the system either by decay or by mass absorption by infected cells. The algebraic term R_F represents the saturation level of type I interferons in the system [19,65,66].

Free virus (V) is produced proportionally to the number of infected cells. This production is reduced by the level of exposure to type I interferons. Viral particles decay naturally, and many are removed during the infection of a single epithelial cell. Free virus is removed by

exposure to antibodies. An additional term is added to model the loss of small numbers of virus by mucous barrier and other factors inhibiting the exposure of virus to epithelial tissue [17].

Uninfected damaged cells (D_H) are the result of elimination of target cells by neutrophil factors; this is modeled as a differential equation. Infected damaged cells (D_I) are the infected cells removed by neutrophil factors, natural killer cells, and CD 8^+ T cells; this is modeled by an algebraic relation assuming that the total number of epithelial cells is constant.

Cytotoxic or CD 8^+ T cells (E) exist naturally at low levels, and are recruited by antigen presenting cells. There is a low level of deactivation proportional to the lysing infected cells. They deactivate on the order of days [67,68].

B cells (B) exist naturally within the system, but they accumulate by maturation of the undifferentiated pool in the presence of immune information given by antigen presenting cells. The maturation of B cells is proportional to the difference between the number of mature B cells and the total pool of cells available to differentiate into B cells, with the process modulated by the cofactor IL-12. In this model plasma cells are not explicitly included, which are B cells that have further differentiated to produce antibodies specific to the virus. B cells are considered removed when they deactivate [67].

Natural killer cells (K) exist endemically within the system, but are mainly recruited by along a chemokine gradient, represented by a Hill function of chemokines. They leave the system either by a natural deactivation or after lysing infected cells [68–72]

Antigen presenting cells (P) exist endemically within the system, but their accumulation starts in earnest when they are exposed to either virus or damaged infected cells. This process is upregulated by type II interferons. For large scale activation, both a source of viral information and type II interferons are necessary; this is represented in the equations by the multiplication of the terms. Antigen presenting cells deactivate on the order of days. Biologically, these can be either dendritic cells or “macrophages”; they are differentiated from

the modeled macrophage class by the presence of cluster-differentiation factor 11c (CD11c+) that helps trigger cellular activation.

IL-12 (W) is a protein produced by antigen presenting cells when they come in contact with Th-1 helper cells (O). Since there are a limited number of receptors to which T_H1 binds, Michaelis-Menten saturation is used to describe their interaction, rather than mass action. An omnibus decay term is used to describe their removal from the system.

Type II interferons (G) are signaling proteins produced primarily by Th-1 helper cells and natural killer cells. Their production is regulated by a saturating function of IL-12. They decay on the order of hours [65,66,69].

Supplement 3: System Parameters and Range

Par	Units	Description	Range	Ref
a_{11}	ml/pg	Signal induced to macrophages by TNF-α	[5.5E-05, 2.2E-02]	[35]
a_{12}	$cells^{-1}$	Signal induced to macrophages by damaged epithelial cells	[4.0E-06, 1.6E-03]	est
a_{21}	dimensionless	Maximal signal induced to macrophages by virus	[1.6E+00, 6.4E+02]	[23]
a_{22}	pfu/ml	Substrate affinity for signal induced by virus	[1.5E+03, 6.0E+05]	[23]
g_1	dimensionless	Inhibitory term for effect of IL-10 on cytokine production	[1.1E+00, 4.5E+02]	est
g_2	pg/ml	Inhibitory term for effect of IL-10 on cytokine production	[3.4E+02, 1.3E+05]	est
δ_2	pg/ml	Inhibitory term for effect of IL-10 on cytokine production	[2.5E+00, 4.0E+02]	[35]
b_{mc}	cells/day	Maximal chemotactic adduction of macrophages	[7.5E+02, 4.1E+04]	[35]
a_{mc}	pg/ml	Substrate affinity for adduction of macrophages	[1.3E+02, 2.0E+03]	[38]
μ_m	day^{-1}	Decay/removal of macrophages	[1.0E-02, 5.0E-01]	[35]
b_m	cells	Baseline number of macrophages	[3.0E+02, 1.2E+04]	[38]
b_t	pg/ml/day	Maximal production rate of TNF-α	[7.8E-02, 3.1E+01]	[35]
k_1	dimensionless	Inhibitory term for pro-inflammatory cytokine production	[2.5E-01, 2.0E+01]	est
k_2	pg/ml	Inhibitory term for pro-inflammatory cytokine production	[2.5E+01, 4.0E+02]	[38]
d_1	pg/ml	Inhibitory term for pro-inflammatory cytokine production	[2.5E+01, 4.0E+02]	[38]
μ_t	day^{-1}	Decay/removal of TNF-α	[2.5E+01, 7.2E+02]	[35]
b_l	pg/ml/day	Maximal production rate of IL-10 by macrophages	[2.1E-02, 8.3E+00]	[35]
μ_l	day^{-1}	Decay/removal of IL-10	[1.8E+00, 1.2E+01]	[35]
b_{lh}	pg/ml/cell	Production rate of IL-10 by target epithelial cells	[5.0E-05, 1.0e-03]	[35]
b_c	pg/ml/day	Maximal production rate of chemokines	[4.0E+00, 1.6E+03]	est
μ_c	day^{-1}	Decay/removal of chemokines	[1.5E+01, 1.8E+02]	[35]
b_{nt}	cells day^{-1}	Maximal activation rate of neutrophils by TNF-α	[4.5E+03, 1.8E+06]	est
a_{nt}	pg/ml	Substrate affinity for activation of neutrophils	[5.0E+00 , 1.6E+02]	[38]
a_{nl}	dimensionless	Inhibitory effect of IL-10 on the activation of neutrophils	[2.5E-02, 1.0E+00]	est
g_{nc}	day^{-1}	Maximal chemotactic adduction of neutrophils	[2.1E+01, 8.4E+03]	est
a_{nc}	pg/ml	Substrate affinity for adduction of neutrophils	[1.8E+01, 7.0E+03]	est
μ_n	day^{-1}	Decay/removal of neutrophils	[1.0E-01, 2.4E+00]	[35]
b_{xn}	pg/ml/day	Maximal production rate of NOS	[1.0E-01, 3.0E+00]	est
a_{xn}	cells	Substrate affinity for production of NOS by neutrophils	[2.0E+02, 8.0E+03]	est
g_{xi}	$cell^{-1}$ day^{-1}	Removal of NOS during infected cell destruction	[1.5E-07, 6.0E-05]	est
g_{xh}	$cell^{-1}$ day^{-1}	Removal of NOS during epithelial cell destruction	[1.5E-07, 6.0E-05]	est
μ_x	day^{-1}	Decay/removal of NOS	[5.0E-01, 1.2E+02]	est
b_h	$cell^{-1}$ day^{-1}	Replication rate of epithelial cells	[1.7E-05, 6.7E-03]	est
θ	cells	Strong Allee term for the replication of epithelial cells	[6.3E+03, 7.5E+04]	est
g_{hv}	ml/pg/day	Viral infection rate	[5.0E-08, 2.0E-05]	[23]
g_{hx}	cells/day	Maximal destruction rate of epithelial cells by NOS	[2.5E-01, 1.0E+02]	est
a_{hx}	pg/ml	Substrate affinity for destruction of epithelial cells	[1.0E-01, 4.0E+01]	est
g_{ix}	cells/day	Maximal destruction rate of infected cells by NOS	[2.5E-01, 1.0E+02]	est
a_{ix}	pg/ml	Substrate affinity for destruction of infected cells	[7.5E-02, 3.0E+01]	est
g_{ik}	$cell^{-1}$ day^{-1}	Removal rate of infected cells by NK cells	[2.5E-06, 1.0E-03]	est

g_{ie}	$cell^{-1}\ day^{-1}$	Removal rate of infected cells by effector cells	[5.0E-6, 2.0E-3]	[23]
μ_i	day^{-1}	Decay/removal of infected cells	[2.5E-01, 4.0E+00]	[23]
g_{vi}	pfu/(ml cells day)	Production rate of virus by infected cells	[7.0E+00, 2.8E+03]	[23]
g_{vh}	$cell^{-1}\ day^{-1}$	Removal of virus during infection of epithelial cells	[4.1E-07, 1.6E-04]	[23]
g_{va}	ml/pfu/day	Elimination of virus due to antibody neutralization	[7.5E-05, 3.0E-02]	[23]
g_v	day^{-1}	Removal rate of sub-threshold viral quantities	[1.4E+00, 5.4E+02]	[23]
a_v	ml/pfu	Inverse of lowest viral level capable of infection	[1.0E+00, 4.0E+02]	[23]
μ_v	day^{-1}	Decay/removal of virus	[5.0E-01, 1.2E+01]	[23]
b_{fi}	pg/(ml cell day)	Production rate of IFN-α/β by infected cells	[2.7E-02, 1.1E+01]	est
b_{fp}	pg/(ml cell day)	Production rate of IFN-α/β by APC	[4.7E-04, 1.9E-01]	est
g_{fi}	$cell^{-1}\ day^{-1}$	Excess absorption rate of IFN-α/β by infected cells	[3.2E-4, 1.3E-01]	est
μ_f	day^{-1}	Decay/removal of IFN α/β	[1.0E+00, 8.0E+01]	[23]
a_{rf}	pg/ml	Substrate affinity of epithelial cells to IFN-α/β	[1.0E+01, 1.4E+02]	[38]
b_k	cells	Baseline number of NK cells	[1.1E+02, 4.6E+03]	[38]
b_{kc}	cells/day	Maximal chemotactic adduction of NK cells	[9.0E+03, 3.6E+05]	[38]
a_{kc}	pg/ml	Substrate affinity for adduction of NK cells	[2.0E+02, 2.0E+03]	[38]
g_{ki}	$cell^{-1}\ day^{-1}$	Removal of NK cells during infected cell elimination	[9.5E-09, 3.8E-06]	est
μ_k	day^{-1}	Decay/removal of NK cells	[4.0E-02, 1.6E+00]	[35]
b_{go}	pg/(ml cell day)	Maximal production rate of IFN-γ by Th1 cells	[7.0E-04, 2.8E-01]	est
a_{go}	pg/ml	Substrate affinity in production of IFN-γ by Th1 cells	[7.5E-01, 3.0E+02]	est
b_{gk}	pg/(ml cell day)	Maximal production rate of IFN-γ by NK cells	[1.7E-02, 6.7E+00]	est
a_{gk}	pg/ml	Substrate affinity in production of IFN-γ by NK cells	[2.3E+00, 9.0E+02]	est
μ_g	day^{-1}	Decay/removal of IFN-γ	[1.0E+00, 8.0E+01]	[23]
P_0	cell/day	Inactive APC available for activation	[1.4E+03, 5.6E+05]	est
g_{pv}	dimensionless	Maximal signal for APC from virus	[1.0E-01, 4.0E+01]	est
a_{pv}	pfu/ml	Substrate affinity for signal from virus	[5.0E+02, 2.0E+05]	est
g_{pi}	$cell^{-1}$	Signal for APC from dead infected cells	[4.8E-06, 1.9E-03]	est
g_p	dimensionless	Non-specific activation rate of APC	[2.5E-03, 1.0E+00]	est
b_{pg}	dimensionless	Maximal activation rate of APC by IFN-γ	[5.7E-02, 2.3E+01]	est
a_{pg}	pg/ml	Substrate affinity for activation of APC by IFN-γ	[4.5E+01, 1.1E+03]	[23]
μ_p	day^{-1}	Decay/removal of APC	[5.0E-02, 9.0E-01]	[23]
b_p	cells	Baseline number of activated APC	[3.0E+02, 9.6E+03]	[38]
b_{ep}	cells/day	Maximal activation rate of effector cells	[1.0E+04, 4.0E+05]	[38]
a_{ep}	cells	Substrate affinity in the activation of effector cells	[1.5E+03, 6.0E+04]	[38]
b_{ei}	$cell^{-1}\ day^{-1}$	Removal of effector cells during infected cell elimination	[7.5E-08, 3.0E-05]	[23]
μ_e	day^{-1}	Decay/removal of effector cells	[1.0E-01, 7.0E-01]	[23]
b_{op}	cells/day	Maximal activation rate of Th1 cells	[2.5E+04, 3.0E+05]	[38]
a_{op}	cells	Substrate affinity in the activation of Th1 cells	[1.5E+03, 6.0E+04]	[38]
μ_o	day^{-1}	Decay/removal of Th1 cells	[1.0E-01, 7.0E-01]	[35]
b_{wo}	pg/(ml cell day)	Maximal production rate of IL-12	[3.8E-03, 1.5E-01]	[38]
a_{wo}	cells	Substrate affinity in the production of IL-12	[2.5E+03, 2.0E+05]	[38]
μ_w	day^{-1}	Decay/removal of IL-12	[5.0E-01, 1.0E+01]	est
b_b	cells/day	Non-specific activation of B cells	[5.0E+00, 2.0E+03]	est
b_{bp}	ml/(cell pg day)	APC induced activation of B cells	[6.0E-08, 2.4E-05]	est
B_0	cells	Reservoir number of unactivated B cells	[1.5E+04, 3.5E+05]	[38]

μ_b	day^{-1}	Decay/removal of B cells	[5.0E-02, 8.0E-01]	[35]
b_a	pg/ml/day	Non-specific production of antibodies	[1.2E-03, 4.6E-01]	[38]
b_{ab}	pg/(ml cell day)	B cell production of antibodies	[3.3E-04, 1.3E-01]	[23]
g_{av}	ml/(pfu day)	Removal of antibodies during virus elimination	[5.0E-07, 2.0E-04]	[23]
μ_a	day^{-1}	Decay/removal of antibodies	[6.0E-02, 1.2E+01]	[23]
H_0	cells	Total number of epithelial cells	2.5E+05	est
h_m	dimensionless	Hill coefficient for the recruitment of macrophages	3	[38]
h_x	dimensionless	Hill coefficient for the inflammatory removal of epithelial cells	2	[38]
h_e	dimensionless	Hill coefficient for the maturation of NKT cells	2	[38]
h_o	dimensionless	Hill coefficient for the maturation of TH1 cells	2	[38]

Table 2: List of model parameters, units, description, upper and lower bounds, and references.

Supplement 4: Metropolis-Hastings Method for Parameter Estimation

As in Battogtokh *et al* [43], the ensemble model is defined to be the system that combines an ODE model, written as $\dot{\mathbf{x}} = \mathbf{f}(\mathbf{x}(t); p)$, with dependent variables $\mathbf{x} = \{x_1, ..., x_{20}\}$ and parameters $\mathbf{p} = \{p_1, ..., p_{94}\}$ (in the order in which they appear in Supplement 3). The associated probability distribution $\rho(p)$ that represents the likelihood that the model captures available data *X,* consisting of a vector of observations $\mathbf{y} = \{y_1, ..., y_n\}$ with standard deviations $\boldsymbol{\sigma} = \{\sigma_1, ..., \sigma_n\}$ and heuristics. Each observation corresponds to a value of a particular variable at a particular time point. A trajectory $\mathbf{x}(t; \mathbf{p}, \mathbf{x}_0)$ of the ODE model with initial condition x_0 is a realization of the random process with the distribution given by $\rho(p)$. Therefore, the value of any variable x_i at any given time is a random variable with the distribution given by $\rho(p)$.

The distribution $\rho(p)$ is estimated using Bayesian inference as the *posterior distribution* $\rho(p \mid X)$ for p, given the data X, by comparing the observed data X with predicted values of the model variables $c(\mathbf{p}) = \{c_1(\mathbf{p}), ..., c_n(\mathbf{p})\}$ that are functions of the trajectory $\mathbf{x}(t; \mathbf{p}, \mathbf{x}_0)$ and hence functions of p. Observational errors are assumed to be normally distributed, and the errors at different time-points are independent; therefore the log-likelihood of observing the data by a model with parameters p given by

$$L(X \mid \mathbf{p}) = \prod_{j=1}^{16} \frac{1}{\sqrt{2\pi\sigma_j^2}} \exp\left(-\frac{(c_j - y_j)^2}{2\sigma_j^2} \right)$$

Bayes formula implies

$$\rho(\mathbf{p} \mid X) = Q^{-1} L(X \mid \mathbf{p}) \theta(\mathbf{p})$$

where $\theta(\mathbf{p})$ is the *prior distribution* based on information available before the data is collected, and $Q = \int L(X \mid \mathbf{p}) \theta(\mathbf{p})$ is the normalizing constant. As the number of parameters is large, the only practical way of describing the posterior distribution is represented by a sample $\mathbf{p}^1, \ldots, \mathbf{p}^M$, i.e. a collection of points on the parameter space distributed according to $\rho(p \mid X)$. This sample is used to estimate the ensemble average of any trajectory-dependent quantity H as

$$\langle H \rangle \cong M^{-1} \sum_{k=1}^{M} H(\mathbf{x}(t; \mathbf{p}^k, \mathbf{x}_0))$$

In addition, using the y -th percentile value of any variable x_j is found as the smallest number that is larger than Y% of values of $x_j(t; \mathbf{p}^k, \mathbf{x}_0)$, $k = 1, \ldots, M$.

For parameters without a well-defined biological range, a Jeffreys distribution is chosen, which is a uniform distribution on a log scale between 1/10th and 10 times a biologically reasonable baseline value. This choice makes posterior distribution scale invariant.

The likelihood function is computed using available clinical data and a set of observations on the response of a naïve host to IAV infection . The known data are the expected values of model variables at time points where the data is available.

Sampling Method for the Ensemble Model

The sample of parameter sets $\mathbf{p}^1, \ldots, \mathbf{p}^M$ (each of which is a vector with 94 components) which represent the posterior distribution $\rho(p \mid X)$ is found $\rho(p \mid X)$ over the parameter space

by using the Metropolis-Hastings Monte Carlo method (MHMC) (sometimes also called Markov Chain Monte Carlo). A formulation is used where it is assumed that $\rho(p \mid X)$ is a Gibbs-Boltzmann distribution derived from some energy function $E(\mathbf{p})$ by the formula $\rho(\mathbf{p}) = \exp(-\beta E(\mathbf{p}))$. The original MHMC method samples the distribution at a fixed value $\beta = 1$ by proposing, at every step k, a random perturbation $\bar{\mathbf{p}}$ of the current parameter set $\mathbf{p}^k$ and accepting this perturbed set as the next set in the sample, i.e. setting $\mathbf{p}^{k+1} = \bar{\mathbf{p}}$, if its energy $E(\bar{\mathbf{p}})$ is smaller than the energy $E(\mathbf{p}^k)$ of the current parameter set. If $E(\bar{\mathbf{p}}) > E(\mathbf{p}^k)$ then the parameter set $\bar{\mathbf{p}}$ is accepted but only with probability $P = \exp(-\beta[E(\bar{\mathbf{p}}) - E(\mathbf{p}^k)]) < 1$ (a random drawing is made for a Bernoulli experiment with probability P and the parameter set is accepted if the drawing results in a success.) If $\bar{\mathbf{p}}$ is rejected then $\mathbf{p}^{k+1}$ is set equal to $\mathbf{p}^k$.

Due to the large dimensionality of the parameter space, the convergence of MHMC is improved using the parallel tempering approach. Parallel tempering algorithm utilizes several replicas of MHMC chains running simultaneously with values of β lower than 1, and produces several output chains $\left\{\mathbf{p}^{1,i}, \ldots, \mathbf{p}^{M,i}\right\}$ where the first index represents the order of the parameter set in a chain, the second index denotes the replica (two superscripts are used so as not to confuse a replica with a component of the vector $\mathbf{p}$). At every step, first the new values of the chain are produced using the standard MHMC method described above, and then the energies corresponding to parameter sets $\mathbf{p}^{k,i}$ and $\mathbf{p}^{k,i+1}$ in two neighboring temperature values β_i and β_{i+1} are compared. If the energy of the high temperature chain, which has a lower beta, is less than that of the low temperature chain, the parameter sets will swap, allowing for a finer exploration of the low energy area. The lower the value of β, the larger the area of the parameter space explored by the chain; therefore, parallel tempering enhances coverage of the parameter space and convergence to the equilibrium distribution. Supplementary figures 1 and

3, which complete figure 2 of the manuscript, displays a simulation of the ensemble model, for initial viral aliquots of 50 and 500 pfus.

Simulation algorithm

1. The starting point $\mathbf{p}^{1,i}$ for each β_i is taken to be the default parameter set.
2. For each β_i and the current state $\mathbf{p}^{k,i}$ compute E_i^k as $E_i^k = -\ln \rho(p^{k,i} \mid X)$ with $\rho(p \mid X)$.
3. For each β_i, generate a new set of parameters $\overline{\mathbf{p}}^i$ according to the proposal density $Q(\overline{\mathbf{p}}^{\mathbf{i}}) = (2\pi\varepsilon_i)^{-1/2} \exp\left(-(\ln \overline{\mathbf{p}}^{\mathbf{i}} - \ln \mathbf{p}^{k,i}) / 2\varepsilon_i\right)$. If any individual parameter value in the new set $\overline{\mathbf{p}}^i$ is above or below the default bounds, that value is rescaled to fit within these limits. (The logarithmic distance and imposed bounds here account for the prior distribution)
4. For each β_i, the energy of the new state is computed as $\overline{E}_i = -\ln \rho(\overline{\mathbf{p}}^{\mathbf{i}})$.
5. For each β_i, $\overline{\mathbf{p}}^i$ is accepted as the new point, $\mathbf{p}^{\mathbf{k+1,i}} = \overline{\mathbf{p}}^{\mathbf{i}}$, with probability $P = \min\left\{1, \exp(-\beta_i(\overline{E}_i - E_i^k))\right\}$. If $\overline{\mathbf{p}}^i$ is rejected then $\mathbf{p}^{\mathbf{k+1,i}} = \mathbf{p}^{\mathbf{k,i}}$.
6. The energies of neighboring chains β_i and β_{i+1} are compared and the parameter sets $\mathbf{p}^{\mathbf{1},i}$ and $\mathbf{p}^{\mathbf{1},i+1}$ are swapped with the probability $P = \min\left\{1, \exp\left((\beta_i - \beta_{i+1})(E_i^k - E_{i+1}^k)\right)\right\}$.
7. Go back to Step 2.

Convergence

Optimal convergence of parallel tempering MHMC is achieved if both the acceptance ratio (i.e, the ratio of accepted to proposed parameter sets) and the swapping ratio are in the range 0.3-0.4. The swapping ratio is controlled by the spacing of β_i (the smaller the spacing the more likely it is for chains to swap). The acceptance ratio is controlled by adjusting the size of the perturbation used in generating $\overline{\mathbf{p}}$. Logarithmic perturbation is used in which the ratio $\overline{p}_j / p_j^k$ for each p is a normally distributed random variable with mean 0 and standard deviation ε.

The acceptance ratio increases with a decreasing value of ε. Convergence of the method is tested on the final distribution by Geweke [73] and Gelman-Rubin tests [74].

Distribution of ensemble objective values

Supplemental Figure 2 represents the ensemble by plotting each parameter combination in the ensemble as a point in the objective space, where the objective values report the relative error of the fit of the trajectory for that parameter combination to either sublethal or lethal data when starting at the appropriate initial condition. There is no single parameter set in the sample that would represent the optimum for both the sublethal and the lethal objectives taken from data across multiple subjects. As is common with multi-objective optimization, the optimization yields a Pareto boundary (shown as black polygonal curve) which represents a collection of parameter sets that cannot be improved in any of the two objectives without degrading the other objective.

Supplement 5: Parameter distributions

Supplementary figure 4 display the full marginal of posterior distribution for model parameters. Yet, survivors and non-survivors are expected to have different parameter distributions. In determining key parameter differences between the survivor (S) and non-survivor (N) ensembles to an initial inoculum of 210 pfu, a direct univariate selection criterion was useless to identify key parametric differences between N and S as all parameters but three were different between ensembles (see table below, yellow highlights). A large number of parameters were also pairwise correlated as expected contributing to the challenge.

Parameter	N		S		p-value*
	Mean	Std. Deviation	Mean	Std. Deviation	
a_11	1.01E-03	9.58E-04	7.46E-04	5.69E-04	4.47E-58

a_12	3.49E-05	2.67E-05	3.29E-05	2.12E-05	2.52E-05
a_21	1.96E+00	1.21E+00	1.81E+00	1.13E+00	4.73E-11
a_22	1.65E+03	6.49E+02	2.16E+03	1.23E+03	1.47E-147
g_1	4.31E+02	1.01E+02	2.89E+02	8.86E+01	0.00E+00
g_2	4.34E+03	1.92E+03	2.96E+03	2.36E+03	4.13E-218
d_2	4.68E+02	9.42E+01	4.13E+02	1.89E+02	6.78E-78
b_mc	1.38E+04	3.86E+03	1.33E+04	3.82E+03	9.36E-11
a_mc	5.05E+02	1.29E+02	5.08E+02	1.23E+02	1.99E-01
mu_m	3.67E-01	1.54E-01	4.99E-01	1.46E-01	0.00E+00
b_m	2.07E+04	2.91E+03	2.01E+04	3.12E+03	1.06E-18
b_t	4.61E+01	1.48E+01	3.80E+01	9.90E+00	1.34E-212
k_1	9.80E-01	2.80E-01	1.59E+00	7.82E-01	0.00E+00
k_2	2.03E+02	5.84E+01	1.18E+02	7.22E+01	0.00E+00
d_1	5.24E+01	5.83E+00	4.54E+01	5.96E+00	0.00E+00
mu_t	6.40E+02	1.93E+02	5.28E+02	2.46E+02	1.57E-138
b_l	1.71E+00	6.67E-01	2.14E+00	1.46E+00	1.45E-80
mu_l	3.94E+00	2.14E+00	5.32E+00	2.18E+00	1.20E-212
b_lh	5.16E-04	1.39E-04	4.78E-04	9.31E-05	2.09E-56
b_c	3.10E+01	1.25E+01	3.02E+01	1.54E+01	4.10E-03
mu_c	1.12E+01	5.05E+00	1.16E+01	3.27E+00	2.75E-06
b_nt	2.02E+06	6.08E+05	2.15E+06	6.43E+05	4.63E-26
a_nt	1.74E+02	3.90E+01	1.55E+02	9.38E+01	2.26E-42
a_nl	5.26E-02	3.80E-02	1.14E-01	1.05E-01	0.00E+00
g_nc	2.27E+03	1.31E+03	1.48E+03	1.50E+03	1.81E-166
a_nc	2.20E+02	7.74E+01	1.09E+02	7.28E+01	0.00E+00
mu_nb	8.28E-01	1.26E-01	7.22E-01	1.62E-01	8.89E-279
mu_n	1.05E+00	6.49E-01	1.23E+00	6.90E-01	4.95E-42
b_xn	1.01E+03	9.14E+02	2.76E+03	2.74E+03	0.00E+00
a_xn	2.83E+04	7.73E+03	4.61E+04	2.06E+04	0.00E+00
g_xi	4.05E-05	1.67E-05	4.29E-05	3.59E-05	5.85E-06
g_xh	1.82E-06	1.15E-05	3.22E-05	4.72E-05	0.00E+00
mu_x	2.10E+02	2.67E+01	1.80E+02	4.14E+01	0.00E+00
b_h	9.06E-05	1.81E-05	6.60E-05	2.63E-05	0.00E+00
theta	1.23E+04	3.18E+03	1.55E+04	7.09E+03	2.39E-183
g_hv	1.08E-06	2.02E-07	6.15E-07	2.70E-07	0.00E+00
g_hx	2.40E+01	1.04E+01	1.22E+01	9.24E+00	0.00E+00
a_hx	1.90E+01	4.39E+00	2.61E+01	1.07E+01	0.00E+00
g_ix	3.57E+00	1.87E+00	1.30E+00	1.01E+00	0.00E+00
a_ix	4.60E-01	3.07E+00	9.01E+00	1.43E+01	0.00E+00
g_ik	7.30E-05	1.05E-04	3.81E-05	8.53E-05	8.36E-72
g_ie	7.84E-04	2.31E-04	5.02E-04	1.37E-04	0.00E+00
mu_i	3.09E+00	1.17E+00	1.74E+00	7.49E-01	0.00E+00

g_vi	3.44E+02	9.69E+01	5.44E+02	2.87E+02	0.00E+00
g_vh	1.28E-05	2.53E-06	1.77E-05	5.34E-06	0.00E+00
g_va	9.04E-04	4.32E-04	1.47E-03	1.26E-03	7.18E-200
g_v	1.72E+02	6.05E+01	2.19E+02	1.81E+02	1.30E-72
a_v	1.07E+01	8.60E+00	2.90E+01	2.70E+01	0.00E+00
mu_v	3.76E-01	5.44E-02	3.07E-01	6.15E-02	0.00E+00
b_fi	2.04E-01	7.11E-02	2.05E-01	9.22E-02	6.33E-01
b_fp	2.22E-01	3.11E-02	1.56E-01	8.04E-02	0.00E+00
g_fi	2.18E-03	1.05E-03	1.38E-03	1.34E-03	1.61E-229
mu_f	1.08E+02	2.49E+01	7.02E+01	2.82E+01	0.00E+00
a_rf	4.90E+01	1.67E+01	8.07E+01	4.86E+01	0.00E+00
b_k	2.38E+02	4.45E+01	2.94E+02	8.82E+01	0.00E+00
b_kc	2.27E+05	6.44E+04	2.61E+05	7.09E+04	2.27E-130
a_kc	1.48E+03	2.89E+02	1.36E+03	2.37E+02	6.34E-107
g_ki	1.20E-08	6.33E-09	2.36E-08	1.90E-08	0.00E+00
mu_k	2.28E+00	3.34E-01	2.34E+00	5.51E-01	3.25E-13
b_go	3.04E-03	3.54E-03	1.24E-02	1.38E-02	0.00E+00
g_go	2.62E-05	1.34E-05	2.99E-05	2.26E-05	1.64E-24
a_go	1.92E+00	8.68E+00	2.44E+01	3.95E+01	0.00E+00
b_gk	1.29E+00	3.72E-01	8.96E-01	1.75E-01	0.00E+00
g_gk	8.38E-05	1.44E-04	6.34E-05	9.50E-05	2.44E-16
a_gk	1.98E+01	9.15E+00	3.14E+01	1.04E+01	0.00E+00
mu_g	7.49E+01	2.54E+01	5.90E+01	1.74E+01	1.25E-265
p_0	6.46E+03	9.78E+03	3.14E+04	4.02E+04	0.00E+00
g_pv	4.66E+01	1.17E+01	2.55E+01	1.69E+01	0.00E+00
a_pv	7.14E+02	2.52E+02	5.43E+02	1.96E+02	1.10E-284
g_pi	2.73E-05	1.14E-05	2.56E-05	1.40E-05	1.42E-11
g_p	2.55E-02	2.96E-02	2.30E-02	2.60E-02	1.28E-05
b_pg	2.70E-01	2.33E-01	3.01E-01	2.40E-01	4.39E-11
a_pg	1.09E+03	4.66E+02	8.95E+02	5.99E+02	1.76E-73
mu_p	4.81E-01	6.64E-02	5.10E-01	8.06E-02	9.47E-88
b_p	2.02E+03	4.37E+02	1.53E+03	4.29E+02	0.00E+00
b_ep	9.98E+04	1.46E+04	8.23E+04	2.16E+04	0.00E+00
a_ep	1.41E+04	2.84E+03	1.10E+04	2.56E+03	0.00E+00
g_ei	3.15E-06	7.68E-06	4.46E-06	7.60E-06	1.66E-17
mu_e	4.25E-01	9.40E-02	5.56E-01	1.23E-01	0.00E+00
b_op	3.48E+05	7.61E+04	2.80E+05	7.82E+04	0.00E+00
a_op	1.58E+04	4.12E+03	1.28E+04	4.98E+03	5.97E-237
mu_o	9.17E-01	1.09E-01	7.37E-01	2.10E-01	0.00E+00
b_w	0.00E+00	0.00E+00	0.00E+00	0.00E+00	1.00E+00
b_wo	9.27E-03	1.64E-03	1.03E-02	2.95E-03	1.57E-111
a_wo	2.45E+03	1.46E+03	1.84E+03	1.17E+03	1.06E-111

mu_w	1.00E+00	2.78E-01	9.59E-01	3.10E-01	3.55E-12
b_b	5.40E+02	1.18E+03	2.61E+02	7.35E+02	2.26E-43
b_bp	1.90E-06	1.32E-06	3.03E-06	1.70E-06	6.35E-288
b_0	5.25E+04	1.30E+04	4.53E+04	1.47E+04	5.31E-145
mu_b	6.03E-01	4.16E-01	6.45E-01	2.79E-01	4.45E-09
b_a	6.74E-03	3.50E-03	3.75E-02	1.56E-01	2.57E-47
b_ab	7.70E-02	2.50E-02	8.65E-02	3.34E-02	1.44E-58
g_av	1.58E-04	3.02E-05	1.07E-04	4.39E-05	0.00E+00
mu_a	4.59E+00	1.37E+00	3.36E+00	9.12E-01	0.00E+00

* 2-sided t-test on a subset of 10,000 parameter sets

We therefore proceeded using L1 and L2 lasso regression, and greedy variable selection using information gain as the selection criteria. The table below display the parameters selected by each of the methods and the rank of selection. We retained parameters selected by at least two of the methods as consistently distinctive between lethal and sublethal ensembles. Because of the very significant correlations, there was a rapid dropoff of significant in multivariate (lasso) regression models. Yellow boxes points to parameters identified by all three methods within the first 14 ranks, while orange boxes points to parameters identified by at least two of the methods in the first 14 ranks. This threshold of considering the first 14 ranks was mostly motivated by the results of the L1 regression and greedy search, which only yielded 11 and 10 parameters in 10-fold cross-validated analysis. L2 lasso (standard ridge regression) is naturally a less parsimonious method and we looked down a few more ranks to see if L2 recovers parameters identified early one by one of the other two methods.

Rank	**Method**		
	L1 lasso	L2 lasso	Information gain
1	b_h	b_h	b_m
2	g_hv	g_hv	a_nt
3	a_mc	a_21	mu_nb
4	g_vh	a_22	b_h
5	b_mc	b_mc	g_hv
6	g_va	a_mc	g_hx

7	a_pv	mu_m	a_hx
8	mu_p	d_1	g_va

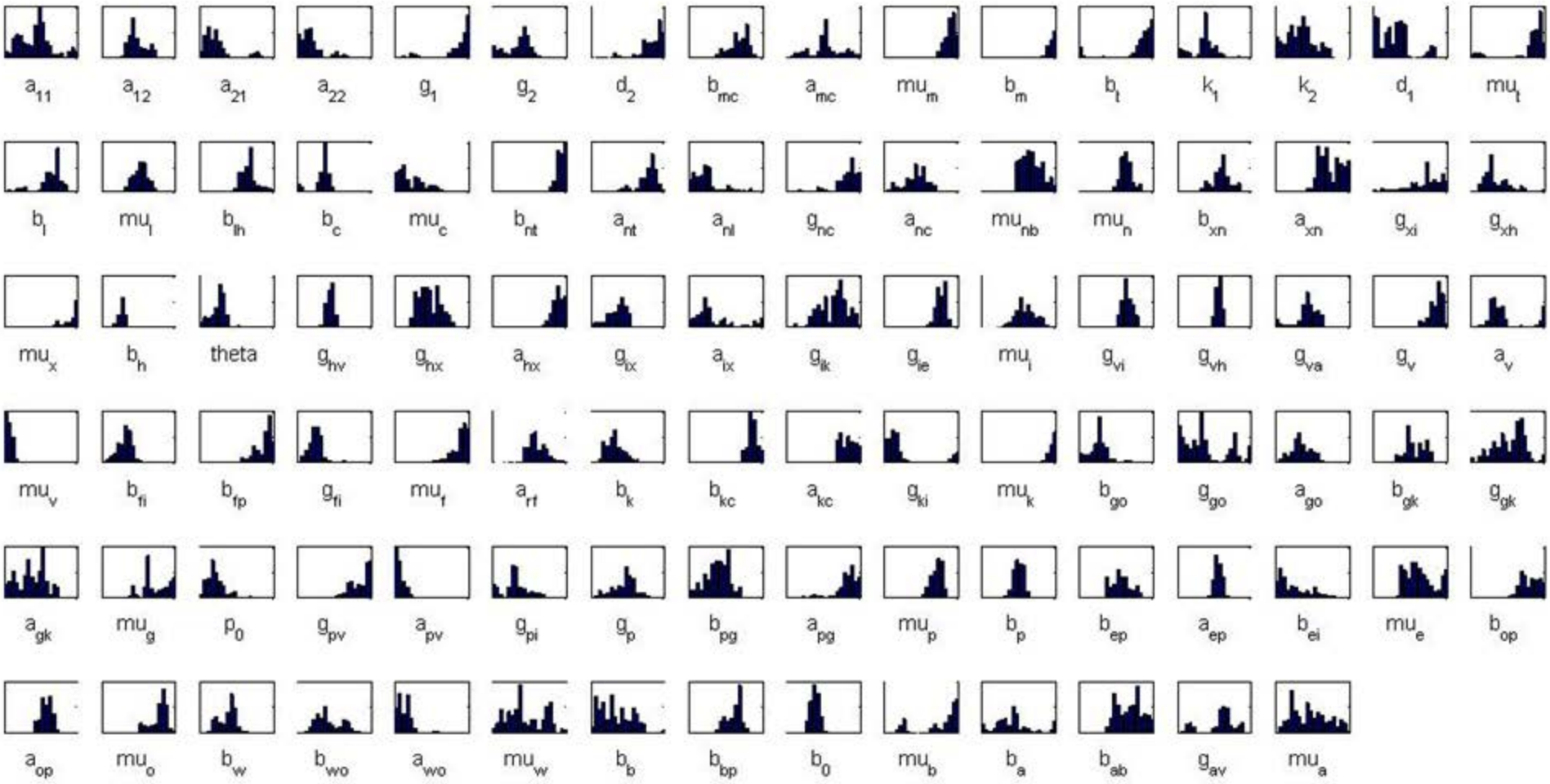

Supplementary Figure 1

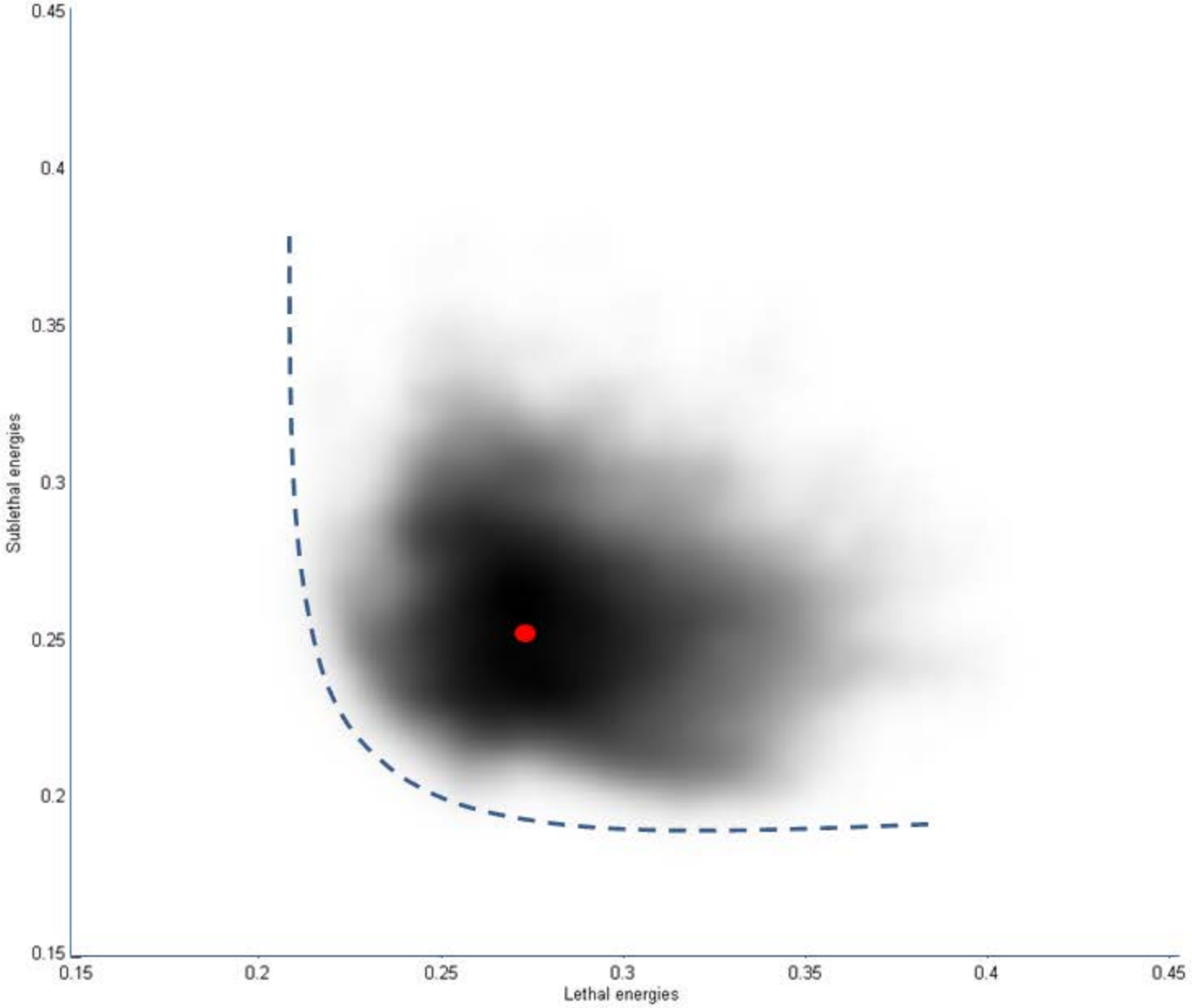

Supplementary Figure 2

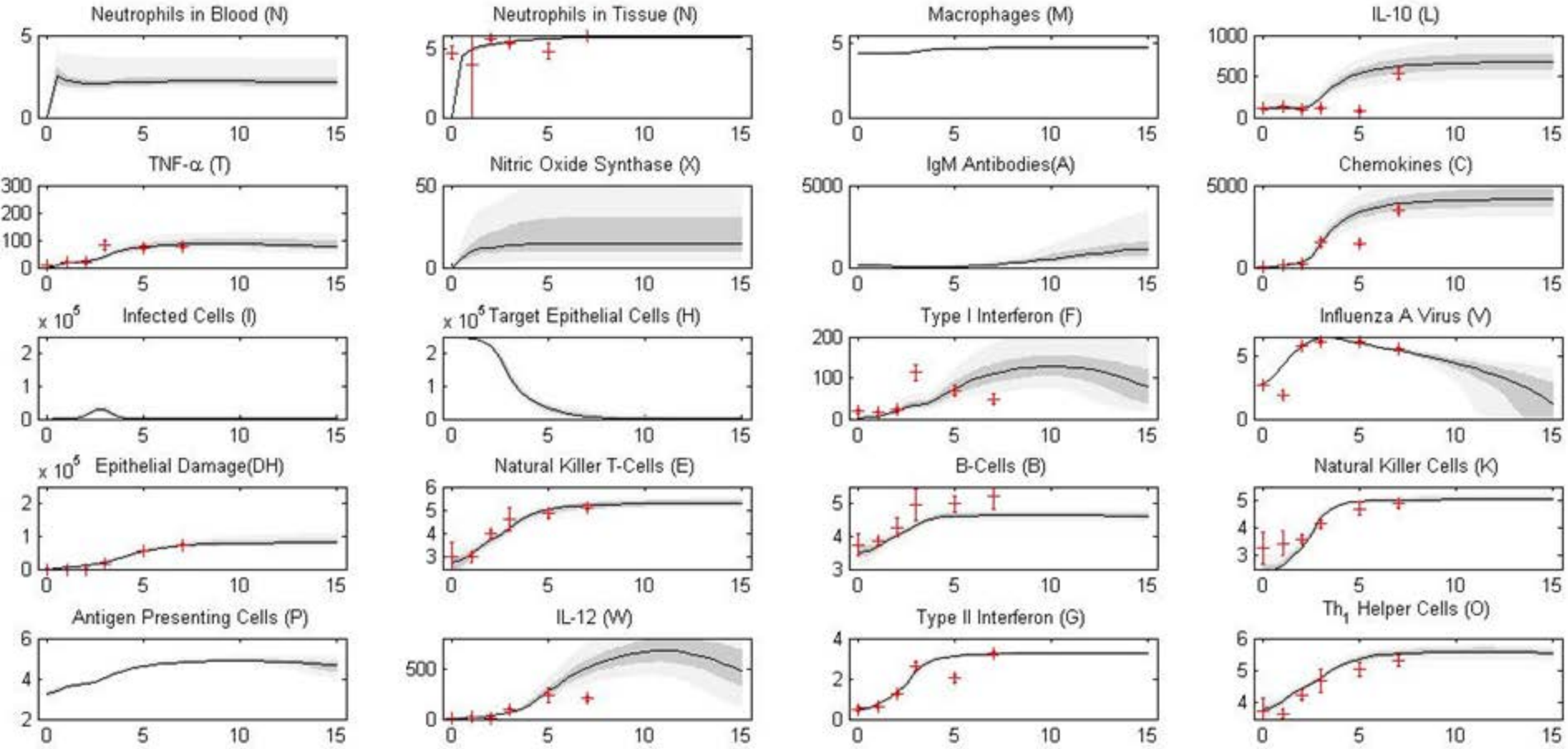

Supplementary Figure 3

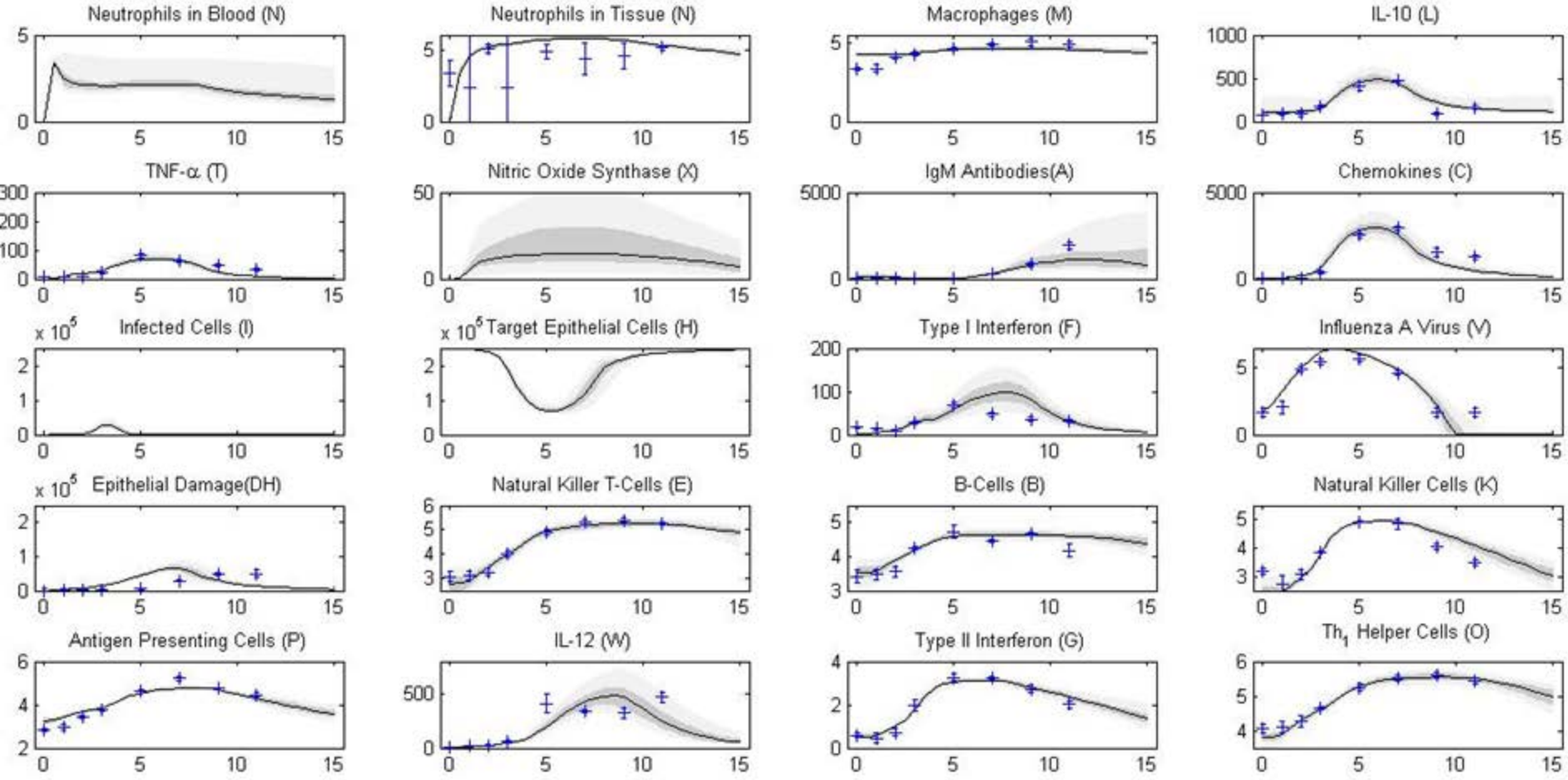

Supplementary Figure 4